Lab on a Chip

CRITICAL REVIEW

Microfluidic fabrication of microengineered hydrogels and their application in tissue engineering

Bong Geun Chung,*[a] Kwang-Ho Lee,[b] Ali Khademhosseini[cdef] and Sang-Hoon Lee*[g]

Microfluidic technologies are emerging as an enabling tool for various applications in tissue engineering and cell biology. One emerging use of microfluidic systems is the generation of shape-controlled hydrogels (*i.e.*, microfibers, microparticles, and hydrogel building blocks) for various biological applications. Furthermore, the microfluidic fabrication of cell-laden hydrogels is of great benefit for creating artificial scaffolds. In this paper, we review the current development of microfluidic-based fabrication techniques for the creation of fibers, particles, and cell-laden hydrogels. We also highlight their emerging applications in tissue engineering and regenerative medicine.

[a]*Department of Bionano Engineering, Hanyang University, Ansan, Korea. E-mail: bchung@hanyang.ac.kr*

[b]*Department of Advanced Materials Science and Engineering, Kangwon National University, Chuncheon, Korea*

[c]*Center for Biomedical Engineering, Department of Medicine, Brigham and Women's Hospital, Harvard Medical School, Cambridge, MA, USA*

[d]*Harvard-MIT Division of Health Sciences and Technology, Massachusetts Institute of Technology, Cambridge, MA, USA*

[e]*Wyss Institute for Biologically Inspired Engineering, Harvard University, Boston, MA, USA*

[f]*WPI-Advanced Institute for Materials Research, Tohoku University, Sendai, Japan*

[g]*Department of Biomedical Engineering, College of Health Science, Korea University, Seoul, Korea. E-mail: dbiomed@korea.ac.kr*

1. Introduction

Tissue engineering is an interdisciplinary field that combines cell biology, biomaterial synthesis, and engineering techniques to generate biological tissue replacements for transplants and tissue culture applications.[1–3] In conventional tissue engineering approaches, cells are seeded onto biodegradable scaffolds that mimic the native extracellular matrix (ECM). Despite major advances in creating a variety of tissue constructs (*i.e.*, cartilage, liver, and bladder), major problems remain,[2,4–6] such as the lack of functional vasculature networks to regulate the transport of nutrients and oxygen, and the inability to control metabolic or mechanical functions of the encapsulated cells within biocompatible scaffolds.[7,8]

Bong Geun Chung

Bong Geun Chung received his bachelors and masters degrees from Hanyang University, Seoul, Korea and his PhD degree from University of California Irvine, USA in 2007. He was an Instructor at Department of Medicine in Harvard Medical School, Boston, USA and is currently an Assistant Professor at Department of Bionano Engineering in Hanyang University, Ansan, Korea. His research interests are in the areas of cell-based biomedical microfluidics, biomaterials-based tissue engineering, and stem cell therapy.

Kwang-Ho Lee

Kwang Ho Lee is an Assistant Professor in the Department of Advanced Materials Science and Engineering at Kangwon National University, Korea. He received the bachelor's (2001) and master's (2003) degrees from Dankook University, Korea. He received a PhD degree (2007) from the Interdisciplinary Program in Medical and Biological Engineering in Seoul National University, Korea. He was a Postdoctoral Associate at the Mechanobiology Laboratory at MIT, USA.

His research interests include the nano and biomaterials-based microstructures for bio-artificial organs and cancer cell research.

Engineered biomaterials that mimic the physical, mechanical, and biological properties of native ECMs may potentially address the challenges of tissue engineering.[3,9–11] Both natural (*i.e.*, collagen, agarose, alginate, chitosan, gelatin, and fibrin) and synthetic (*i.e.*, poly(acrylic acid), poly(ethylene oxide)-derived hydrogels, *etc.*) biomaterials have been widely used.[10,12] These hydrogel-based biomaterials can be crosslinked by various methods, such as by the addition of chemical chelators, ultraviolet (UV) light, and temperature.[13] The swelling, degradation, wettability, porosity, and gelling conditions of hydrogels play a significant role in controlling their physical, mechanical, and diffusive properties. Hydrogel degradation is important for regulating controlled drug release and the viability of transplanted cells. To create biodegradable scaffolds, various conventional tissue engineering approaches have been previously used.[14] For instance, biodegradable poly(glycolic acid) (PGA) fibers have been utilized to create three-dimensional (3D) porous scaffold structures that could significantly improve cell adhesion and growth.[15] Non-bonded fibers were encapsulated within a matrix and were selectively dissolved by thermal treatment to yield highly porous structures. To generate an open porous biodegradable matrix, a gas foaming technique has also been developed.[16] For example, poly(D,L-lactic-*co*-glycolic acid) (PLGA) and salt particles were compressed in a high CO_2 gas pressure environment. The particles encapsulated within the PLGA matrix leached, thereby generating pores. The size of the pores created by gas foaming and salt leaching methods was controlled by the salt particle size. Similar salt fusion approaches have been used to generate interconnected pores within an engineered scaffold.[17] The interconnected pores created by the salt fusion method could control the mechanical compressive modulus. Given the diffusive properties of the interconnected pores, the salt fusion technique might be useful for enhancing cell growth and migration. Although the conventional tissue engineering approaches (*i.e.*, gas foaming, salt leaching) can generate

porous biodegradable scaffolds, these methods have limitations, such as the use of high gas pressure and organic solvents that may damage cells. Furthermore, cells on these scaffolds often see a two-dimensional (2D) environment as they are seeded on a substrate, compared to being encapsulated in a 3D environment.

Microfabrication techniques have been employed to create artificial tissue constructs comprising microfibers, microparticles, and hydrogel building blocks.[2,18] Microfibers can be directly used as a scaffold, whereas hydrogel building blocks can be used to create tissue building blocks.[19–21] Microfluidic devices fabricated by photo- and soft-lithographic approaches can be used to fabricate microvascularized networks embedded within 3D polymeric microfibrous structures, which improve the delivery efficiency of drugs, nutrients, and oxygen. Thus, the merging of microfabrication techniques and biomaterials is a potentially powerful approach for mimicking native tissue architecture. In this paper, we review various microfluidic-based polymerization techniques (*i.e.*, chemical, photo, and thermal polymerization) for creating fibers, particles, and cell-laden hydrogels and also discuss their application in tissue engineering (*i.e.*, co-culture, microvasculature, scaffold, and tissue assembly) (Table 1).

2. Microfluidic fabrication

2.1. Microfluidic synthesis of microfibers

Hydrogel-based microfibers created by laminar flow-based multiple phase coaxial flowing systems are of benefit for creating tissue scaffolds. To generate hydrogel-based microfibers, the conventional spinning technique has been previously used. For example, a triple-orifice spinneret was employed to generate hollow and solid fibers of gelatin-hydroxyphenylpropionic acid (Gtn-HPA) hydrogels.[22] The diameters of the hollow and solid fibers were manipulated by the flow rates. Gelatin-based fibers are beneficial for creating tissue engineered scaffolds, because

Ali Khademhosseini

Ali Khademhosseini is an associate professor affiliated with the Brigham and Women's Hospital and Harvard Medical School. He also directs a satellite laboratory at the WPI-AIMR at Tohoku University. He has authored over 170 papers in peer reviewed journals and numerous other works. He has received numerous major awards including the United States Presidential Early Career Award for Scientists and Engineers, the Pioneers of Miniaturization award and the Technology Review Magazine TR35 award. He received his PhD in bioengineering from MIT, and MASc and BASc degrees from University of Toronto both in chemical engineering.

Sang-Hoon Lee

Sang-Hoon Lee is professor in the department of Biomedical Engineering at Korea University. He received a BS degree in electrical engineering and MS and PhD degrees in biomedical engineering from the Seoul National University in Korea, 1983, 1987 and 1992, respectively. From 1992 to 2006, he was Professor in the Department of Biomedical Engineering at the Dankook University. His current interests are the development of microfluidic devices to provide microenvironment for cell study and tissue engineering, microfluidic fiber and capsule fabrication for bioartificial organ, and flexible implantable sensor for biomedical applications. In addition, he is very interested in 2D and 3D microenvironment control for cell study based on microfluidic technology.

Table 1 Microfluidic fabrication techniques for tissue engineering applications

Microfluidic fabrication	Polymerization	Biomaterial	Tissue engineering approach (size of microfabricated structure)	Ref.
Microfiber synthesis	Chemical	Alginate	Co-axial flow-based microfiber (20–50 μm)	24
			Microfibers derived from cylindrical microchannels (75–115 μm)	27
			Hollow microfiber-based microvascularized channel to co-culture endothelial cells and smooth muscle cells (50–200 μm)	59
		PLGA	Microfiber for aligning fibroblast cells (10–242 μm)	25
		Chitosan	Core–sheath flow-derived microfiber for creating artificial liver (70–150 μm)	26
			Microfiber to co-culture Schwann cells and fibroblast cells (50–200 μm)	60
		PPDO-*co*-PCL-*b*-PEG-*b*-PPDO-*co*-PCL	Porous microfiber to culture fibroblast cells and analyze mitochondrial activity (2–200 μm)	28
	Photo	4-HBA, PVA	"On the fly" photocrosslinkable microfiber (20–90 μm)	29
		Polyurethane	Janus microfibers for enhancing cell adhesion and mechanical strength (100 μm)	30
Microparticle formation	Photo	4-HBA	Monodisperse hydrogel microparticle (70–250 μm)	32
			Hydrodynamic-based cell encapsulation (75–250 μm)	33
		TMPTA	Self-assembled amphiphilic microparticle fabricated by continuous flow lithography (103 μm)	35
		pNIPAAm	Monodisperse microparticle for gel emulsification (70–200 μm)	36
		PEG	Continuous flow lithography technique-based multifunctional microparticle (10–30 μm)	37
			Stop-flow lithography-based cell-laden microgels (100 μm)	38
			Self-assembled magnetic hydrogel microparticle (30–43 μm)	39
			Self-assembly of micro-train hydrogel building blocks (100 μm)	77
		Silica	Raspberry-like monodisperse microparticle (80–140 μm)	40
		TPGDA	Monodisperse microparticle in a flow-focusing microfluidic device (20–1000 μm)	41
		PBA-PAA	Monodisperse double emulsion (50–500 μm)	42
		PLGA	Double emulsion with hollow and porous structures (300–350 μm)	43
		HR4	Double emulsion in a microfluidic device treated with hybrid inorganic/organic polymer coatings	44
		PFPE, AHPCS	Inorganic–organic Janus microspheres for drug delivery (164 μm)	45
		Acrylamide	Monodisperse hydrogel Janus granules (56–90 μm)	46
	Chemical	Alginate	Microparticles derived from cylindrical microchannels (130–400 μm)	27
			Monodisperse hydrogel microbead for cell encapsulation (100–140 μm)	34
Microfluidic hydrogel system	Thermal	Agarose	Cell-laden microfluidic device	50
			Microporous cell-laden microfluidic device	51

Table 1 (*Contd.*)

Microfluidic fabrication	Polymerization	Biomaterial	Tissue engineering approach (size of microfabricated structure)	Ref.
		Gelatin, Pluronic	Microfluidic hydrogel networks with gelatin meshes	54
		PGS	A microfluidic device with ridge-grooved channels to regulate cellular alignment	55
			Albumin production of hepatocytes cultured on microvascularized channel	63
		Collagen	3D microfluidic device for *in situ* ECM phase interface	56
			Effect of cAMP on microvascularized channel (120 μm)	66
			Effect of mechanical environment on function of microengineered vessels (120 μm)	67
			Tumor cell invasion in a 3D co-culture microchannel (400 μm)	70
			Tumor cell migration in response to the interstitial flow in a microfluidic device	71
			Modular tissue assembly with HepG2 cells and fibroblast cells (300 μm)	76
		Silk fibroin	Liver function in silk fibroin microchannels (90–240 μm)	68
	Chemical	Alginate	Overlapping concentration gradients in a 3D microfluidic scaffold	69
	Photo	Methylated hyaluronic acid, collagen	Microfluidic semi-interpenetrating network channel (300 μm)	57
		PEGDA	Cell-encapsulated multilayer microfluidic vascularized channel	58

gelatin is a natural material with which cells can interact as it is derived from collagen and contains adhesive RGD peptides. To generate pores within these fibers, Gtn-HPA or alginate fiber was selectively removed by treating the resulting microfibers with collagenase or sodium citrate. Cells were encapsulated within the inner core of these fibers, which was covered by a hydrogel outer shell, showing that cells cultured in the inner core tended to migrate toward the outer layer. Hollow microfibers have also been created using a similar spinning method.[23] In this approach, the inner diameter of the alginate hollow fibers was controlled by a coaxial triple fluid flow (core: 10% (w/v) dextran, sample: 1% (w/v) alginate, and sheath: 100 mM $CaCl_2$). Furthermore, L292 fibroblast cells were encapsulated within the hollow alginate microfibers to enable the formation of tubular tissue constructs. However, the conventional spinning methods have some limitations, such as the inability to generate symmetric or asymmetric Janus microfibers containing different pore size or mechanical stiffness. To address the limitations imposed by the conventional spinning techniques, microfluidic devices have been recently used to fabricate hydrogel microfibers. Such microfabrication techniques have enabled the generation of biomimetic microfibers that resemble the native ECM structures, such as those of collagen fibers.

2.1.1. Co-axial flow-based microfiber. Co-axial flow-based microfluidic devices have been widely used to generate microfibers containing various shapes and sizes. For example, calcium alginate microfibers have been generated in a microfluidic platform.[24] This approach used a poly(dimethylsiloxane) (PDMS)-based co-axial flow microfluidic device containing a capillary glass pipette. Solid alginate fibers were generated using the sample flow of 2% (w/v) sodium alginate solution and the sheath flow of a 100 mM $CaCl_2$ solution. The diameter of the resulting alginate fibers could be modulated by controlling the fluidic flow velocity. As the flow rates of the alginate increased, the fiber diameter was also increased. The utility of this approach in tissue engineering applications was demonstrated by encapsulating cells and proteins within microfibers.

Co-axial fluid flow has also been used to generate fibers from other materials, such as PLGA, which is a degradable polymer that is often used for tissue engineering scaffolds. PLGA fibers generated in a microfluidic device have been used to control cellular orientations with their defined diameters.[25] This work demonstrated that cellular orientation of mouse fibroblast cells, as defined by the angle between the axis of cells and long axis of fibers, was directly related to the diameter of the fibers. In particular, the diameter of microfibers enabled the control of the mean orientation of cells, showing that the cellular orientation increased with decreased fiber diameters. Such microscale fibrous networks have great potential to generate tissues with aligned cellular orientation or to guide the migration of cells. In another example, co-axial flow-based chitosan microfibers have been synthesized in a microfluidic device (Fig. 1A).[26] The diffusion coefficient (7.8×10^{-8} cm^2 s^{-1}) within the synthesized chitosan

microfibers was quantitatively measured using the fluorescence recovery after the photobleaching (FRAP) technique. Human hepatocarcinoma (HepG2) cells cultured on pure chitosan microfibers showed higher liver-specific functions, such as albumin and urea synthesis, potentially due to the presented glycosaminoglycans that could enhance cell adhesion. Recently, a cylindrical microchannel-based platform has been used to generate microfibers without glass capillary tubes.[27] Co-axial flows were simultaneously modulated in 12 rectangular microfluidic channel mixers formed by convex hemi-cylindrical SU-8 microchannels. The sheath (CaCl$_2$) and sample (alginate solution) flows enabled the control of the continuous synthesis of alginate microfibers without clogging. This approach was used to generate microfibers with various compositions in a parallel manner, providing a potentially useful tool for scaling up the microfiber fabrication process for tissue engineering applications.

2.1.2. Porous microfiber. The porosity within microfibers plays an important role in controlling the delivery of nutrients and oxygen. Pores within microfibers can be created by a variety of approaches, such as the use of porogens or through the solvent exchange process. As an example, amphiphilic triblock copolymer-based porous microfibers have been fabricated in a microfluidic device and subsequently processed to generate porous fibers (Fig. 1B).[28] Porous microfibers of amphiphilic triblock copolymer, poly(p-dioxanone-co-caprolactone)-block-poly(ethylene oxide)-block-poly(p-dioxanone-co-caprolactone) (PPDO-co-PCL-b-PEG-b-PPDO-co-PCL), were generated by the immersion precipitation and solvent evaporation methods. The diffusion-based mass exchange between a polymer solution and a non-solvent stream generated pores within the microfibers. The amphiphilic triblock copolymer-based porous microfiber was used to encapsulate proteins and drugs, showing that the rate of protein release was increased with the degree of porosity. Also interestingly, mouse fibroblast cells that were cultured on these microfibers had increased mitochondrial activity as the microfiber diameters were decreased.

2.1.3. Photocrosslinkable microfiber. Photocrosslinkable hydrogels have also been processed into fibers by using a microfluidic-based platform.[29] For example, 4-hydroxy butyl acrylate (4-HBA) and polyvinyl alcohol (PVA) solutions were used to create photocrosslinkable microfibers in a flow-based microfluidic device. As expected, the diameters of the resulting microfibers decreased with increased sheath flow rates. As 4-HBA is pH-sensitive, the elongation of microfibers was strongly affected by pH changes. Photopolymerization has also been used to fabricate Janus polyurethane microfibers in a microfluidic device (Fig. 1C).[30] The asymmetric Janus polyurethane microfibers contained two types of compartments, such as porous and non-porous regions. The porous regions of the Janus microfibers enhanced cell adhesion, whereas the mechanical strength was higher in the non-porous regions.

2.2. Microfluidic particle formation

Microfabrication techniques have been recently used to generate microparticles with various sizes and shapes.[31] For instance, polymeric microparticles have been developed by *in situ* photo-polymerization techniques.[32] In one example, a photocrosslinkable hydrogel/enzyme solution and an immiscible oil solution were used in a pressure-derived microchannel as a sample and sheath flow, respectively. To generate hydrogel particles, two fluids were merged at the tip of the glass micro-pipette and were subsequently crosslinked by a UV light. The picoliter microparticles were formed by the surface tension and shear forces generated at the junction of the microfluidic channel. This process resulted in the formation of monodisperse micro-particles that could be manipulated by controlling the flow rates. As the sheath flow rates increased, the resulting particles were smaller. Microcapsules can also be generated in a continuous and cost-effective manner by combining hydrodynamics and *in situ* photopolymerization.[33] For example, pH-responsive microcap-sules (*i.e.*, 4-HBA, PVA) were generated by the transient flow in a microfluidic device.[33] When the core fluid broke up inside the sample stream, the thread-like jet of the sample fluid was stabilized within the sheath stream, showing that the shells could protect the encapsulated materials. Given their ability to encapsulate various chemicals and cells in monodisperse and shape-controlled particles, these microfluidic platforms hold great potential for generating delivery vehicles for various types of applications.

In addition to photocrosslinkable microparticles, mono-disperse alginate microbeads have been chemically crosslinked in a microfluidic device (Fig. 2A).[34] Sodium alginate with calcium carbonate (CaCO$_3$) nanoparticle and corn oil with lecithin were delivered to "T"-shaped microchannels to create microdroplets. Calcium carbonate nanoparticles allowed the gelation of microgels, showing that calcium ions reacted with sodium alginate within the microdroplets in a microchannel. The size of the alginate hydrogel microbeads was controlled by adjusting the flow rate and the aspect ratio of the microbeads decreased with increasing flow rates. Jurkat cells were encapsulated inside alginate hydrogel microbeads (100–140 μm in diameter) with higher cell viability.

2.2.1. Flow lithography technique-based microparticles. The flow lithography technique has been developed in a microfluidic device to generate microparticles. For instance, the continuous flow lithography technique has been used to synthesize amphiphilic wedge-shaped microparticles by photocrosslinking immiscible polymeric precursors (*i.e.*, hydrophobic tri(methylol propane triacrylate) (TMPTA) and hydrophilic poly(ethylene glycol) diacrylate (PEGDA)) in a Y-junction microchannel.[35] The polymerized amphiphilic microparticles were self-assembled in water or water–oil two phase interfaces. Photocrosslinkable poly(N-isopropylacryamide) (pNIPAAm)-based monodisperse microparticles have also been generated by combining pre-gel emulsification.[36] To form microparticles, pNIPAAm precursors and crosslinking solutions were emulsified and were subsequently dispersed through a microchannel. The polymer-analogous reactions could provide particle formation derived from the polymer synthesis. This method could be performed by gradually varying the degree of crosslinked particles for applications of functionalized sensors or actuators.

The continuous flow lithography technique has been used to create complex patterns or multi-functional particles in
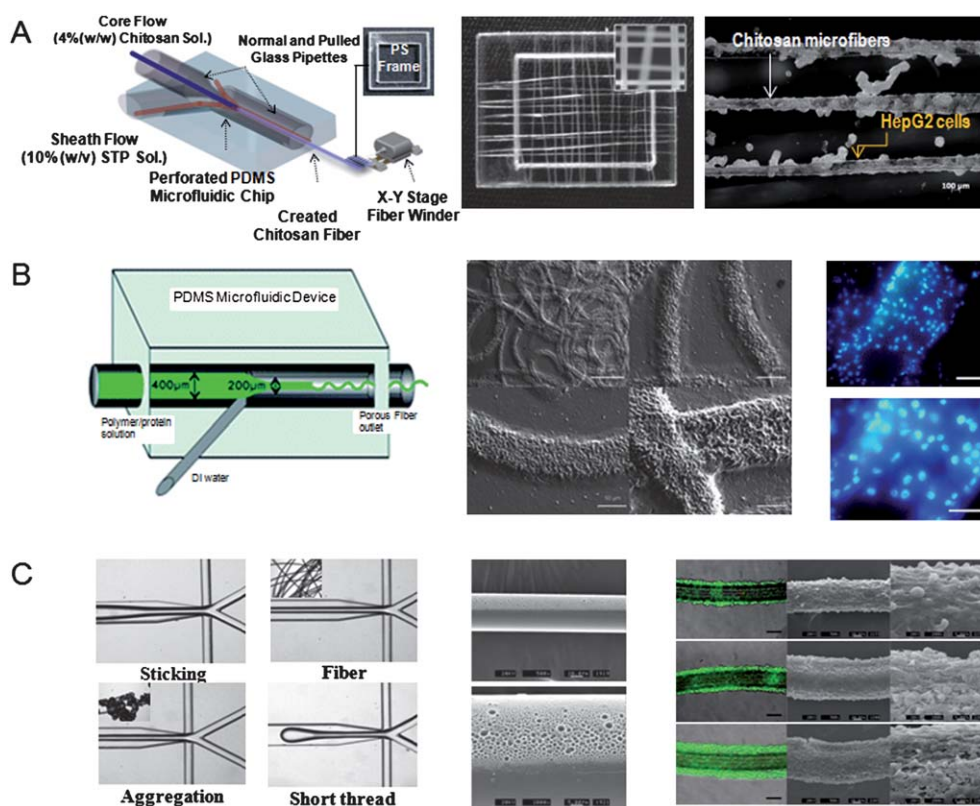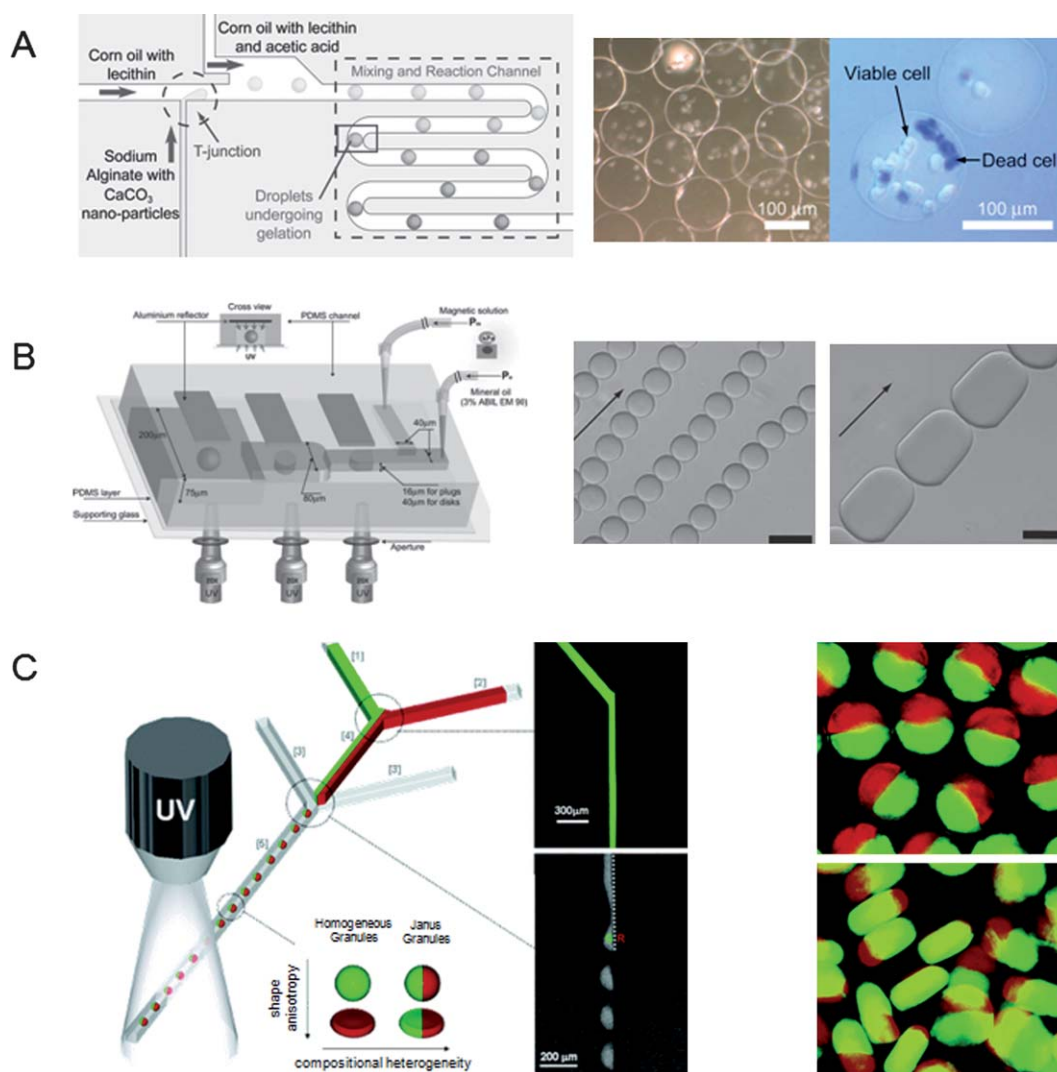
Fig. 1 Microfibers fabricated in a microfluidic device. (A) Chitosan microfibers created in a microfluidic device. Scanning electron microscope (SEM) image of chitosan microfibers. HepG2 cells cultured for 5 days on the chitosan microfibers. (Reprinted with permission from ref. 26, Copyright 2010 The Royal Society of Chemistry.) (B) Amphiphilic triblock copolymer-based porous microfibers. SEM and fluorescent images show the porous microfibrous scaffolds and fibroblast cells cultured on microfibers for 5 days (blue indicates DAPI stained cell nucleus). (Reprinted with permission from ref. 28, Copyright 2010 The Royal Society of Chemistry.) (C) Polyurethane Janus porous microfibers that are photopolymerized in a microfluidic device. SEM images show porous microfibers and fibroblast cells adhered onto the surfaces of microfibers. (Reprinted with permission from ref. 30, Copyright 2009 The Royal Society of Chemistry.)

a microfluidic platform with a throughput of nearly 100 particles per second.[37] This technique has been used to fabricate functional microparticles that could be useful for generating 3D hydrogel microarchitectures in a rapid and high-throughput manner. For example, bi-functional rectangular-shaped Janus microparticles containing rhodamine-conjugated PEGDA streams were continuously synthesized at the interface of the co-flowing microfluidic device due to the laminar flow and photo-polymerization. It was observed that UV exposure times decreased with increasing the thickness of microchannels and feature sizes of patterned mask films. The stop-flow lithography technique has also been used to create cell-laden hydrogel microparticles.[38] Unlike the continuous flow lithography system, fluidic flows containing PEGDA precursors and fibroblast cells were stopped and were subsequently photocrosslinked by a UV light through a mask thin film containing various shapes. Although n-vinyl pyrrolidone (NVP) enhanced the photo-initiation reaction, the viability of the cells encapsulated within hydrogels was decreased, showing that the cell viability was inversely proportional to PEGDA or photo-initiator concentrations. It was revealed that shorter UV exposure times played an important role in improving the throughput and controlling robust shapes of cell-laden hydrogels. Thus, stop-flow lithography enabled the generation of cell-encapsulated PEGDA

microparticles with higher cell viability. Furthermore, spherical or non-spherical magnetic hydrogel microparticles have been synthesized in a T-Junction microfluidic device (Fig. 2B).[39] Magnetic nanoparticles with superparamagnetic properties were homogeneously encapsulated inside hydrogels in a microfluidic device containing aluminium reflector, which could provide both multi-directional UV exposure and higher UV energy flux to create non-deformed spherical hydrogels. The self-assembling of particles was controlled by a vibrating sample magnetometer, showing that the hydrogels were preferentially aligned when the external magnetic field was applied. This system has several advantages over previous synthesis techniques, such as continuous production of particles and high particle monodispersity.

2.2.2. Emulsion-based microparticles. Monodisperse emulsion-based microparticles generated in a microfluidic device could be potentially useful for cell encapsulation and controlled drug release. For instance, the spherical monodisperse microparticles have been generated in a microfluidic device.[40] To fabricate colloidal silica particles, co-axial glass capillaries were inserted into a microfluidic device to generate photocurable emulsion droplets. The synthesized silica particles were partially exposed from the ethoxylated trimethylolpropane triacrylate (ETPTA) matrix with a silane coupling agent for selective

Fig. 2 Microparticles fabricated in a microfluidic device. (A) Monodisperse alginate hydrogel microbeads for cell encapsulation. (Reprinted with permission from ref. 34, Copyright 2007 John Wiley & Sons, Inc.) (B) Schematic of the magnetic hydrogel microparticle fabrication. SEM images show the self-assembly of magnetic microparticles with sphere (left) and plug (right) shapes. Scale bars are 25 μm. (Reprinted with permission from ref. 39, Copyright 2008 The Royal Society of Chemistry.) (C) Schematic of Janus colloid-filled hydrogel granules. Fluorescent images show the Janus spherical (top) and discoidal (bottom) granules. (Reprinted with permission from ref. 46, Copyright 2006 American Chemical Society.)

functionalization. A raspberry-like surface morphology was created by removing the silica particles from the ETPTA matrix. The complex patterns on the microparticles might be useful for biochemical screening and colloidal barcoding applications. Monodisperse microdroplets have been created in a flow-focusing microfluidic device.[41] Tripropyleneglycol diacrylate (TPGDA) microdroplets containing different sizes (*i.e.*, 20–1000 μm) and shapes (*i.e.*, sphere, rod, disk, and ellipsoid) were generated in a narrow orifice in which two immiscible liquids merged. Multi-component polymeric microbeads with 4 nm CdSe quantum dots were generated in a flow-focusing micro-fluidic device. Thus, this microfluidic hydrodynamic flow-focusing system enabled the fabrication of microdroplets that were derived from either polymerization of liquid monomers or thermal solidification.

Monodisperse double emulsions with core–shell microstructures have also been photocrosslinked in a capillary microfluidic device that was consisted of cylindrical glass capillary tubes.[42] The diblock copolymer, poly(butyl acrylate)-*b*-poly(acrylic acid) (PBA-PAA), was used to generate water-in-oil-in-water double emulsions (50–500 μm in diameter) within single droplets. The amphiphilic polymers were subsequently self-assembled in a microfluidic device when solvent was evaporated. It was observed that the droplets were formed by the dripping and jetting process, showing that dripping made the drops at the entrance of the collection tube and jetting was formed by viscous stress of the outer fluid. The droplets of double emulsions are of great benefit for applications of encapsulation or controlled release of various drugs. Furthermore, biodegradable PLGA microbeads containing hollow and porous microstructures have been generated in a microfluidic capillary device.[43] The emulsion-templated PLGA microbeads (300–350 μm in diameter) were fabricated in the water-in-oil-in-water phase of a flow-based microfluidic device. In this process, a polymeric surfactant (*i.e.*,

PVA) was employed to stabilize the double emulsions. Emulsion templating and the rapid evaporation of organic solvents enabled the generation of highly porous structures. It was observed that average diameter of droplets was inversely proportional to flow rates of the inner water phase. This approach has the potential to create interconnected pores that can facilitate the delivery of nutrients and oxygen to cells. These emulsion-based microfluidic devices are useful tools for encapsulating cells and controlling drug release.

The surface cleaning and chemical modification of the polymer also plays an important role in regulating the surface property of the microfluidic device. To generate double emulsion droplets in a PDMS microfluidic device, hybrid inorganic/organic polymer (i.e., HR4) has been used to improve the resistance of microchannels.[44] HR4 (1.5 μm in thickness) was coated on PDMS microchannels, followed by UV irradiation and thermal curing. It was observed that the double emulsion droplets were created in a HR4-modified microfluidic device without any swelling. This HR4-based chemical modification made the surface hydrophilic, reduced the rate of solvent absorption, and minimized the air trapping problem in microchannels. Fourier-Transform Infrared (FT-IR) spectrum analysis showed that Si–OH groups, formed between HR4 and PDMS surfaces, increased the strength of the covalent bonding. This chemical modification approach enables the control of solvent-resistance of microfluidic devices to create double emulsion droplets.

2.2.3. Janus microparticles. Janus microparticles containing multiple biochemical functions have been recently generated in a microfluidic device. Monodisperse inorganic–organic Janus microspheres have been created in a microfluidic device.[45] Functionalized hydrophobic perfluoropolyether (PFPE) and hydrophilic allylhydridopolycarbosilane (AHPCS) was used as an organic and inorganic phase, respectively. The monodisperse microparticles were photocrosslinked at the junctions of the microchannels where AHPCS, PFPE, and 2% sodium dodecyl sulfate (SDS) solutions were applied. These Janus microspheres resulted from a shear-force-driven break-off mechanism, which could form four different shapes, such as unstable, dumbbell, symmetric, and asymmetric. Thermal decomposition of the PFPE region and oxidative removal of the organic component altered the microsphere morphology from a dumbbell shape to a mushroom shape, yielding silicon-oxycarbide-based ceramic hemispheres. Furthermore, the microspheres were aligned and rearranged under an external magnetic field, when magnetic nanoparticles (Fe_3O_4) were applied to the inorganic AHPCS phase. The homogeneous monodisperse hydrogel Janus granules have also been fabricated in a sheath-flow microfluidic device (Fig. 2C).[46] Acrylamide hydrogel-based colloidal microspheres were generated in an oil phase and were subsequently photopolymerized inside the microfluidic device to immobilize the colloids inside the droplets. This in situ photopolymerization process enabled the control of non-spherical or heterogeneous granules. The analysis of the processing phase diagram showed that the poly-disperse droplets were formed at a high silica concentration and granule adhesion was generated at a low acrylamide concentration. Thus, the microfluidic device enabled the control of colloid-filled Janus granules with controlled sizes and shapes.

2.2.4. Micromolding technique-based microparticles. The micromolding techniques have been previously used to generate shape-controlled hydrogel microparticles.[47,48] For instance, cells were suspended in PEGDA or methacrylated hyaluronic acid hydrogel solution and were subsequently placed on a hydrophilic PDMS microstamp treated with oxygen plasma.[47] The cell-encapsulated hydrogel microparticles with various shapes (i.e., square, disk) were hydrated and harvested from a PDMS microstamp after UV exposure. This simple micromolding technique enabled the generation of the checkerboard patterning of hydrogels encapsulated with fibroblast cells and mouse embryonic stem cells. Despite the potential of the micromolding technique, the major challenge still remains, such as rapid gelling derived from direct contact with gelling agents. To address this limitation, chemically crosslinkable hydrogels (i.e., alginate) and the controlled-release of the gelling agent (i.e., calcium ion) have been used to create cell-laden microparticles.[48] The microtransfer molding technique showed that alginate was micromolded on calcium-containing patterned agarose substrates and was subsequently crosslinked by calcium ions released from the agarose, resulting in the formation of fibroblast cell-laden hydrogel microparticles. The mechanical properties of cell-laden hydrogels might be regulated by hydrogel precursor concentrations and the multilayer structures could be created using the sequential replica micromolding. This microtransfer molding technique is a powerful approach for achieving the controlled release of drugs and proteins.

2.3. Microfluidic hydrogel systems

2.3.1. Temperature-sensitive engineered hydrogel. Microfabrication techniques enable the generation of the cell-laden microfluidic hydrogel systems. Temperature-sensitive hydrogels obtained from natural (i.e., agarose, gelatin, collagen, fibrin, and Matrigel) materials have been widely used to generate the microfluidic-based tissue architectures. For example, a cell-laden agarose, a polysaccharide derived from red algae,[49] microfluidic system has been previously developed.[50] An agarose gel-based microfluidic device has been fabricated by the micromolding technique, showing that the agarose surfaces and agarose-based microfluidic devices were bonded upon heating at 71 °C. The diffusion profiles of molecules within 3D agarose gels were analyzed by fluorescent-conjugated bovine serum albumin (BSA), indicating that fluorescent-conjugated BSA inside a microchannel diffused into agarose gels. The cells were encapsulated within the agarose gel microfluidic devices and their viability in microchannels was investigated with respect to the distance from the microchannels. Quantitative analysis showed that the viability of cells exposed to the medium flow was higher as compared with phosphate buffered saline (PBS) flow or no flow conditions, because flow-derived nutrients were efficiently delivered to the cells encapsulated within the agarose gels.

Agarose gels have also been used to create microporous cell-laden microchannels.[51] Micropores within hydrogels played an important role in controlling the diffusion of the molecules, however, previous approaches for creating pores have used toxic chemicals, showing the inability of generating cell-encapsulated hydrogel structures.[52] To overcome this limitation, agarose-based microporous cell-laden systems have been developed by

the sucrose-leaching process. Cell suspension, agarose, and sucrose crystals were mixed at 40 °C and were subsequently poured into a PDMS mold containing a microchannel. Agarose gels have been polymerized during the rapid cooling process and sucrose crystals were dissolved by leaching from the microgels in a homogeneous manner, resulting in creating micropores without noticeable cell damage. The pore type was controlled by the sucrose concentration, indicating that the pores were interconnected at higher sucrose concentrations. The mechanical stiffness and cell viability of microporous agarose gels were also investigated, showing that the mechanical stiffness decreased at higher sucrose concentrations and the cell viability decreased at larger distances from the microchannel surfaces.

Medium transport plays an important role in enhancing cell viability and metabolic function in a hydrogel.[53] To enhance medium transport through the hydrogels, gelatin has been used as a sacrificial material for creating a microfluidic hydrogel network platform.[54] Gelatin meshes were generated using a PDMS micromolding technique. Briefly, an ethylene oxide-propylene oxide-ethylene oxide co-polymer (*i.e.*, Pluronic) was introduced into oxidized PDMS channels and liquid gelatin was subsequently applied into microchannels. After gelation of the gelatin, the gelatin mesh was easily separated from the microchannels, because gelatin did not adhere to the Pluronic substrate. These gelatin meshes were also encapsulated within various temperature-sensitive hydrogels (*i.e.*, collagen, Matrigel) to create microfluidic hydrogel systems with open network microchannels. Furthermore, biodegradable poly(glycerol sebacate) (PGS)-based micro/nanopatterned substrates (>500 nm in width) have been used for cell guidance.[55] Ridge-grooved substrates on sucrose-coated PGS micropatterns were generated by a deep reactive etching method to regulate cellular orientation and alignment. Quantitative analysis showed that the cells cultured on ridge-grooved substrates were more aligned and elongated than those cultured on flat PGS surfaces, showing that cells cultured on flat surfaces were randomly oriented. The cell alignment was calculated by measuring the angles between the long axes of the cells and the direction of the micro/nanopatterns. Thus, this PGS-based micro/nanopatterned substrate might be potentially useful to generate *in vivo* implantable devices for studying cell–cell interactions and cellular alignments.

Microfabrication techniques have been used to create 3D ECM-based platforms.[56] Natural ECM biomaterials (*i.e.*, collagen, fibrin, and Matrigel) have been used to assemble *in situ* 3D hydrogel matrices in a microfluidic platform with a phase interface separated by the flow of two ECM precursors (Fig. 3). Collagen fibers nucleated and assembled from the collagen-doped alginate phase interface, although they did not assemble from the pure alginate phase interface. To investigate whether the collagen-alginate phase could regulate the morphology of the encapsulated cells, alginate was uncrosslinked in the presence of sodium citrate. It showed that the fibroblast cells were more elongated in the uncrosslinked alginate-collagen matrix than in the crosslinked alginate-collagen matrix. This approach that can enable the control of the 3D ECM phase interface has the potential for assembling the collagen fibers and analyzing the motility of the encapsulated cells within the 3D ECM matrix.

2.3.2. Photocrosslinkable engineered hydrogel. Photopolymerization methods have been previously used to create cell-laden microfluidic hydrogel systems. Hyaluronic acid, which is a component of the ECM, has been used to create the microfluidic hydrogel system.[57] The methylated hyaluronic acid was synthesized with collagen to form semi-interpenetrating networks. The mechanical properties of the collagen-methylated hyaluronic acid interpenetrating networks showed that compressive moduli and fracture stresses were proportional to the methylated hyaluronic acid concentrations. Cell viability analysis showed that mouse embryonic fibroblast cells, which were encapsulated within microfluidic collagen-methylated hyaluronic acid microchannels, remained viable (>70%). Synthetic materials have also been used to create a microfluidic hydrogel platform. For example, PEGDA has been used to develop a multi-layer cell-laden microfluidic hydrogel platform (Fig. 4).[58] Flow-based PEGDA microfluidic channels that could regulate pressure-based convective transport were generated by using PDMS micromolding techniques. It demonstrated that the nutrient and waste mass transport enabled the control of cell viability and scaffold metabolic density in a temporal and spatial manner. It was also revealed that molecular diffusivity was significantly decreased with increasing molecular weights and PEGDA concentrations. This may be because the pore size decreased at high PEGDA concentrations. As expected, the cell viability was significantly regulated by the nutrient diffusion, showing that the viability of the fibroblast cells near the medium perfusion microchannels was higher as compared with cells at the peripheral regions (600–1500 μm distance from microchannels) of the device. Thus, this multi-layer soft lithographic method enabled the control of the molecular diffusion profiles and cell viability in microvascularized channels.

3. Tissue engineering applications

3.1. Cell-laden microfibers

Microfibers fabricated in microfluidic devices are of great interest for use in culturing a variety of cell types. For instance, the co-axial microfluidic device with 3 inlets (core: 100 mM $CaCl_2$, sheath: 2% alginate solution, and sample: 100 mM $CaCl_2$) has been used to synthesize endothelial cell-laden alginate hollow fibers (Fig. 5).[59] The hollow microfibers were wound on a cover glass, suggesting the feasibility to align the hollow fibers. It was observed that molecules were immobilized inside the alginate hollow microfibers and the releasing profiles of chemokines were measured for analyzing the nutrient transportation. To mimic a human vascular vessel, human iliac vein endothelial HIVE-78 cells were immobilized in an alginate hollow fiber that was co-cultured with smooth muscle cells. This approach that can synthesize the cell-laden or protein-immobilized hollow microfiber is of great benefit for studying the vascular morphogenesis. To create the chitosan microfiber derived from hydrodynamic focusing, a poly-methyl-methacrylate (PMMA) microfluidic chip with cross-junction microchannels has also been developed.[60] The cross-junction microchannel was used to induce crosslinking reaction by chitosan solution and sodium tripolyphosphate solution. The chitosan microfibers coated with collagens, which could facilitate the culturing of Schwann cells and fibroblast
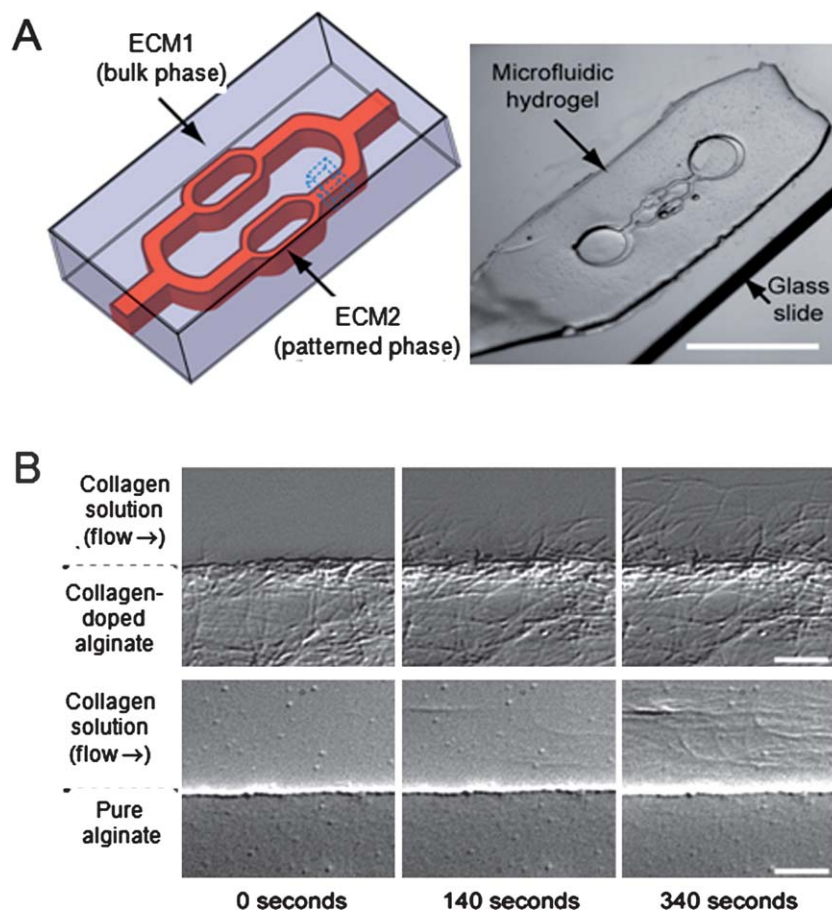
Fig. 3 *In situ* assembly of collagen fibers in a 3D microfluidic matrix. (A) Schematic of a microfluidic 3D hydrogel matrix device. (B) Time-lapse images of the collagen fiber assembly at the two-phase interface. (Reprinted with permission from ref. 56, Copyright 2008 Macmillan Publishers Limited.)

cells, were 50–200 μm in diameter. It was controlled by the ratio of the core to the sheath flow. In addition to microfluidic-based microfibers, the conventional spinning method has been used to generate highly porous and biodegradable gelatin-hydroxy-phenylpropionic acid (Gtn-HPA) hydrogel hollow microfibers for immobilizing Madin–Darby canine kidney (MDCK) and human microvascular endothelial (HME) cells.[61] A solution containing Gtn-HPA and mixed cell suspension was polymerized under the laminar flow with diffusion of the enzymatic oxidative reactants in a triple-orifice extruder that could form a triple-layered co-axial laminar flow. The arbodiimide/active ester-mediated coupling reaction and enzymatic oxidative reaction of the HPA moieties was employed to conjugate Gtn-HPA hydrogels. Thus, this system enabled the generation of the single or dual-layered Gtn-HPA hydrogel fibers and co-cultured with MDCK and HME cells as a model for blood vessels.

3.2. Microvascularized microfluidic hydrogels

The microfabrication technique enables the generation of microvascularized structures that have the potential to create functional endothelialized networks. For example, polystyrene-based microvascular bifurcated networks have been generated in a microfluidic device containing semi-circular microchannels.[62] Primary human umbilical vein endothelial cells (HUVECs) were

cultured inside semi-circular microchannels that were generated by the electroplating process. HUVECs were adhered to bifurcated microchannel networks to form lumen structures. Endothelialized networks have also been generated in PDMS-based
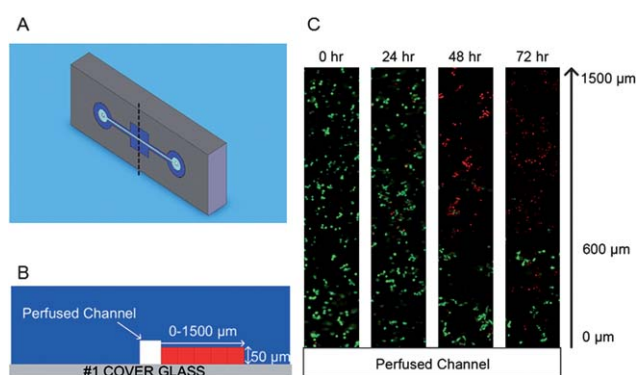

Fig. 4 Cell-encapsulated multilayer microfluidic hydrogel device. (A) Schematic of the PEG microchannel. (B) Cross-sectional schematic of the hydrogel microchannel. (C) Confocal fluorescent image showing the viability of the fibroblast cells encapsulated within a PEG hydrogel microfluidic device with as a function of the distance from the perfusion channel (0–1500 μm, green: viable cell, red: dead cell). (Reprinted with permission from ref. 58, Copyright 2010 Elsevier.)

microfluidic devices.[7] Human microvascular endothelial cells were cultured for 2 weeks in flow-based bifurcated microfluidic network channels. The immunostaining analysis of the endothelial cell markers (*i.e.*, CD31 and von Willebrand factor (vWF)) showed that the cells formed as a monolayer within the microchannels and expressed vascular proteins. A biodegradable polymer-based microfluidic device has also been created to model multilayer vascular networks.[63] PGS, a synthesized biodegradable elastomer, was used as a 3D scaffold material to culture hepatocytes. Sucrose, a sacrificial layer, was spin-coated on a silicon master patterned with microchannels and PGS was subsequently micromolded from the silicon master. It was observed that hepatocyte aggregates were easily formed from higher cell density. Albumin production of hepatocytes cultured in a medium perfusion-based microfluidic device was analyzed to evaluate hepatic function, showing an albumin production rate of 24.3 μg cm^{-2} per day. The main advantage of this approach is that hydrogels can be bonded without any toxic solvent. Therefore, microfabrication techniques and engineered hydrogels are of great benefit for creating 3D tissue engineered scaffolds containing microvascularized networks.

The second messenger cyclic adenosine monophosphate (cAMP) enables the control of the barrier function of blood microvessels.[64,65] To investigate the effect of cAMP on barrier function of microvessels where human dermal microvascular blood endothelial cells were formed, a collagen gel-based microfluidic platform with open network microchannels has been used.[66] The perfusion analysis of fluorescent-conjugated BSA demonstrated that the microvessels without cAMP were more permeable and showed local leaking, whereas microvessels with higher concentrations of cAMP prevented the permeation of a fluorescent-labeled BSA solution. It was revealed that cAMP decreased the permeability and local leaking, whereas it increased the charge selectivity and mechanical stability of the engineered microvessels, resulting in enhanced microvascular barrier function. Cell proliferation and apoptosis assays showed that higher concentrations of cAMP inside the engineered microvessels suppressed the cell division and apoptosis. Thus, a collagen-based microfluidic system provides a powerful method for studying the effect of cAMP on microengineered vessels. Similar collagen-based microfluidic platforms have been used to investigate the effect of mechanical microenvironments on the function and phenotype of engineered microvessels.[67] Quantitative analysis showed that high flow rates enhanced the barrier function and vascular stability of engineered human microvessels, showing that the flow increased vascular diameter, decreased the permeability, and eliminated the focal leaking. In addition to vascular barrier function, the fluidic flow was used to control the vascular phenotype. Tapered tubes or parallel tubes were used to investigate the effect of the shear stress on the vascular phenotype. Vascular endothelial-cadherin (VE-cadherin) immunostaining results indicated that lower shear stress
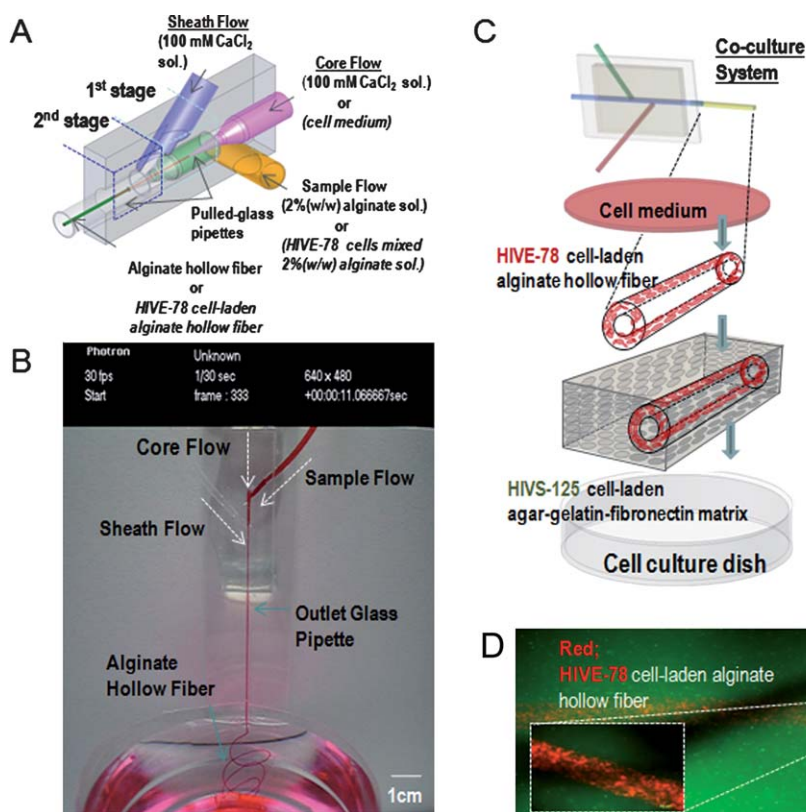
Fig. 5 Microfluidic device for fabricating the microvascularized microfibers. (A) Schematic of the microfluidic device to generate alginate hollow fibers. (B) Micrograph of the hollow fiber generation process involving co-axial flows (*i.e.*, core, sample, and sheath flow). (C) Embedding alginate hollow fibers for co-culture. (D) Cell tracking images of co-cultured HIVE-78 and HIVS-125 cells. (Reprinted with permission from ref. 59, Copyright 2009 John Wiley & Sons, Inc.)

generated in the wide microchannels of a tapered tube increased the disorganization of cell–cell junctions. Thus, the collagen gel-based microfluidic platform enables the control of the vascular functions and phenotypes. Furthermore, cell-laden silk fibroin microfluidic devices have been developed for culturing HepG2 cells over 5 days.[68] The micromolding technique-based silk fibroin microchannels were generated by bonding between the water-stable silk fibroin layers in an aqueous silk solution to create multi-stacked microvascularized channels. The liver-specific function and mechanical properties of fibroin were investigated, showing that the albumin secretion of HepG2 cells cultured in perfusion-based silk fibroin microfluidic devices increased after 3 days. Quantitative analysis of the mechanical strength showed that the mechanical strength and toughness of the silk fibroin was higher as compared with PGS.

3.3. Microfluidic scaffolds

3D microfluidic scaffolds have been recently developed to control cellular functions. For instance, a microfluidic scaffold has been developed to control extracellular microenvironment.[69] Soft lithography techniques enabled the encapsulation of the cells inside a calcium alginate-based 3D microfluidic scaffold system that could generate concentration gradients in a temporal and spatial manner. The overlapping concentration gradients were stably generated within a 3D microfluidic scaffold platform. The diffusion-reaction process, which was confirmed by controlling the spacing of microchannels, showed that the convective mass transfer played an important role in regulating the metabolic environment. This 3D microfluidic scaffold platform that can mimic the native tissue microarchitectures enables the control of the drug delivery in a temporal and spatial manner. A 3D multi-cellular co-culture system has been developed in a microfluidic culture device to study cell–cell and cell–matrix interactions in a real-time manner.[70] Two parallel microchannels were connected into the gel channel containing the post arrays. In a microfluidic device, metastatic breast cancer cells and RAW macrophage cells were encapsulated within collagen I and Matrigel, respectively. It demonstrated that macrophage cells invaded into the breast cancer cell-laden hydrogels. The surface tension and wettability played a significant role in regulating the filling process of hydrogels in the gel channel, indicating that hydrophobic gels were patterned within the gel channel in a spatial manner. This platform, which enables the control of 3D co-cultures of multiple cell-laden hydrogels inside the juxtaposed microchannel, provides a powerful method to engineer cell–microenvironment interactions. The migration of tumor cells in response to the interstitial flow has also been investigated in a microfluidic culture device containing a 3D collagen I gel matrix.[71] It demonstrated the effect of the interstitial flow on cancer cell behaviors, showing that the interstitial flow enabled the control of the direction of the tumor cell migration. Although the cells cultured in control devices without the flow migrated randomly, the cells exposed to the interstitial flow migrated along the flow streamline in a microfluidic device. Interestingly, when the CCR7 receptor of breast cancer cells was blocked, the cells migrated toward upstream or against the flow. This study demonstrated the effect of CCR7-depednet or independent chemotaxis in a 3D microfluidic culture device. Furthermore, the

microsyringe deposition and soft lithography techniques enabled the fabrication of PLGA scaffolds.[72] PLGA solutions were deposited by pressure-assisted microsyringes and soft lithography techniques (*i.e.*, micromolding, microfluidics, and spin coating) were used to fabricate 3D PLGA scaffolds. The microsyringe technique enabled the control of PLGA scaffolds in an automatic manner and the soft lithography method played an important role in fabricating multi-layer polymeric scaffolds. These rapid prototyping techniques enable the fabrication of microscale polymeric 3D scaffolds with well-defined geometries.

A porous micropatterned scaffold has been fabricated for creating vascular tissue engineering applications.[73] The porous micropatterned PCL scaffolds were created using soft lithography, melt molding, and particulate leaching of PLGA particles. This study demonstrated that the nutrient was highly diffused through the porous PLGA-leached scaffolds as compared with non-porous scaffolds. It was revealed that vascular smooth muscle cells were aligned on micropatterned PLGA-leached PCL scaffolds without the loss of the cellular organization. In contrast, the cells cultured on un-patterned and non-porous PCL scaffolds were not aligned. This micropatterned cell sheet enables the fabrication of tissue engineered blood vessels with physiological vessel functions and well-defined bifurcated vessel structures. The surface modification of hydrogels is of great benefit for tissue engineering applications. For instance, ephrin-A1 and Arg-Gly-Asp-Ser (RGDS), cell integrin ligand, have been covalently immobilized on the surface of PEG hydrogels using photopolymerization.[74] This has been used to demonstrate that ephrin-A1, a key factor of vascular development, enhanced the adhesion of endothelial cells through $\alpha_v\beta_3$ integrin. Also, endothelial tubules were created on the ephrin-A1 immobilized PEGDA hydrogel surface. Thus, immobilization of ephrin ligands played an important role in controlling angiogenic functions. Furthermore, to determine the function of the positional context, the mammary epithelial tubules have been engineered using the 3D collagen micropatterning technique.[75] The mammary branching morphogenesis could be controlled by various growth factors or extracellular matrix molecules. This study demonstrated that multi-cellular branches were extended into the surrounding collagen, when the epidermal growth factor or hepatocyte growth factor was applied. It was observed that primary mammary epithelial cells were polarized to form bilayered tubules and tubule branches were inhibited by increasing concentrations of inhibitors, which were released from epithelial cells. This *ex-vivo* lateral tree-like branch system is of great interest in investigating the morphogenesis of mammary epithelial cells and primary organoids.

3.4. Hydrogel building block-based tissue assembly

Hydrogel assembly is of great interest in creating native tissue microstructures. A microfluidic platform has been used to spatially assemble hydrogels containing different cell types (Fig. 6A).[76] Cylindrical-shaped collagen modules containing fibroblast cells and HepG2 cells were assembled in a narrow microchannel. Medium perfusion through the cell-laden collagen gels in a microfluidic device enabled the control of modular tissue shapes, showing that the shape of the collagen module was changed at higher flow rates. After medium perfusion, the
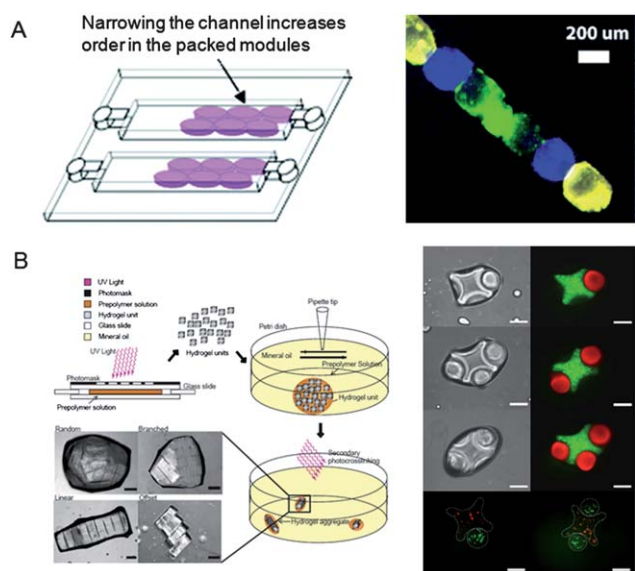
Fig. 6 Hydrogel building block-based tissue assembly. (A) Modular tissue constructs in a microfluidic device. The assembled cell-laden gels with different fluorescent dyes. (Reprinted with permission from ref. 76, Copyright 2008 The Royal Society of Chemistry.) (B) Directed assembly of the cell-laden hydrogel building blocks derived from the two-phase interface and bottom-up tissue engineering technique. Fluorescent images show the lock-and-key-shaped hydrogel assembly. Scale bars are 200 μm. (Reprinted with permission from ref. 78, Copyright 2008 The National Academy of Sciences.)

collagen modules were retrieved from the microchannels. Thus, this microfluidic-based modular tissue assembly system has the potential to create hierarchical tissue architectures, encapsulate multiple cell types within collagen gels, and perfuse culture medium into cell-laden collagen gels. Furthermore, hydrogel building blocks have been assembled in a railed microfluidic device.[77] The railed microfluidic device containing microgrooved channels enabled the control of individual UV crosslinkable hydrogel building blocks, resulting in creating self-assembly of microgel blocks in an accurate and rapid polymerization manner. The polymerized PEGDA microgels moved along the grooved microchannels to create 2D self-assembled micro-train structures. This rail-based microfluidic platform enabled the generation of the self-assembled microgels and manipulated the micropatterning of different cell types (i.e., HeLa, HEK 293 cells). These microfluidic-based microgel assembly techniques play an important role in creating tissue assembled microarchitectures.

Hydrogel building blocks have been recently assembled using photolithography and bottom-up engineering techniques. For instance, cell-laden individual building blocks of PEG hydrogels containing various shapes (i.e., square, lock-and-key shape) have been assembled to create the tissue architectures (Fig. 6B).[78] Briefly, a PEG solution was placed on a glass substrate and was subsequently exposed to a UV light through a shadow mask film containing various micropatterns, resulting in generating individual building blocks of PEG hydrogels. Hydrophilic PEG microgels were assembled in the hydrophobic oil phase due to the surface tension at the oil–water interface. Despite its potential for generating the assembled tissue architectures, this method is limited in that the individual building blocks of PEG hydrogels were assembled by using manual mechanical agitation. To overcome the problem of manual mechanical agitation, perflurodecalin, which was more hydrophobic than mineral oil, has been used to create self-assembled hydrogel structures.[79] Individual building blocks of hydrophilic PEG hydrogels moved toward each other and were self-assembled on the hydrophobic perflurodecalin solution due to low surface free energy and surface tension on the air–liquid interface. The capillary forces also enabled the control of the individual building blocks to minimize the free surface area, resulting in forming capillary force-driven self-assembled tissue-like microarchitectures. Their assembly behavior was controlled by the stirring speed and time. However, the approaches described above were inherently 2D and therefore it was difficult to use them to create 3D mesoscale tissue-like constructs. To address this limitation, a micromasonry assembly process has been developed.[80] Individual building blocks of hydrogels were placed on a PDMS template and the excess pre-polymer solution was subsequently removed to induce the assembly. During this process, mesoscale 3D tissue-like structures were created by attaching individual building blocks of PEG hydrogels to a PDMS surface with cylindrical-shapes due to the capillary force. When hydrophilic PEG building blocks were placed in a hydrophobic solution before the photopolymerization process, the efficiency of the hydrogel self-assembly was significantly improved. After the photopolymerization process, the PDMS template was removed to generate hepatocyte-laden hydrogel assembly structures with hollow tube-like shapes. These approaches are of great interest in creating artificial assembled tissue architectures, because in vivo tissue is mainly consisted of small repeating subunits of hydrogels.

4. Conclusions and future directions

The microfluidic fabrication technique is of great benefit for various tissue engineering applications, such as co-culture, microvasculature, and tissue assembly (Table 1). Given the recent development of microfabrication techniques and engineered functional biomaterials, the implantable cell-laden microfluidic devices containing multiple biological functions may be developed for regenerating self-assembled tissue constructs without any cell damage or immune response. Despite advancements in the development of microfabrication and microscale tissue engineering techniques, some limitations that prevent the use of tissue engineering applications still remain, such as the inability to create large-scale tissue constructs containing microvascularized network channels and the lack of controlling over long-term cell survival and function. These limitations may be addressed by development of high-throughput 3D microfluidic scaffold platforms containing nanoparticles conjugated to target ligands or microfiber-based microvascularized networks that can be used to create mesoscale tissue-like constructs. Therefore, the merging of microfluidic fabrication techniques and engineered functional biomaterials can be a potentially powerful approach to create 3D cell-laden self-assembled tissue constructs containing multi-layer microfiber-based microvascularized networks.

Acknowledgements

References

1 R. Langer and J. P. Vacanti, *Science*, 1993, **260**, 920–926.
2 A. Khademhosseini, R. Langer, J. Borenstein and J. P. Vacanti, *Proc. Natl. Acad. Sci. U. S. A.*, 2006, **103**, 2480–2487.
3 A. Khademhosseini and R. Langer, *Biomaterials*, 2007, **28**, 5087–5092.
4 K. Kojima, L. J. Bonassar, A. K. Roy, H. Mizuno, J. Cortiella and C. A. Vacanti, *FASEB J.*, 2003, **17**, 823–828.
5 K. M. Kulig and J. P. Vacanti, *Transplant Immunol.*, 2004, **12**, 303–310.
6 A. Carraro, W. M. Hsu, K. M. Kulig, W. S. Cheung, M. L. Miller, E. J. Weinberg, E. F. Swart, M. Kaazempur-Mofrad, J. T. Borenstein, J. P. Vacanti and C. Neville, *Biomed. Microdevices*, 2008, **10**, 795–805.
7 M. Shin, K. Matsuda, O. Ishii, H. Terai, M. Kaazempur-Mofrad, J. Borenstein, M. Detmar and J. P. Vacanti, *Biomed. Microdevices*, 2004, **6**, 269–278.
8 J. T. Borenstein, E. J. Weinberg, B. K. Orrick, C. Sundback, M. R. Kaazempur-Mofrad and J. P. Vacanti, *Tissue Eng.*, 2007, **13**, 1837–1844.
9 N. A. Peppas, J. Z. Hilt, A. Khademhosseini and R. Langer, *Adv. Mater.*, 2006, **18**, 1345–1360.
10 J. L. Drury and D. J. Mooney, *Biomaterials*, 2003, **24**, 4337–4351.
11 B. K. Mann, *Clin. Plast. Surg.*, 2003, **30**, 601–609.
12 K. T. Nguyen and J. L. West, *Biomaterials*, 2002, **23**, 4307–4314.
13 B. V. Slaughter, S. S. Khurshid, O. Z. Fisher, A. Khademhosseini and N. A. Peppas, *Adv. Mater.*, 2009, **21**, 3307–3329.
14 K. R. King, C. C. J. Wang, M. R. Kaazempur-Mofrad, J. P. Vacanti and J. T. Borenstein, *Adv. Mater.*, 2004, **16**, 2007–2012.
15 A. G. Mikos, Y. Bao, L. G. Cima, D. E. Ingber, J. P. Vacanti and R. Langer, *J. Biomed. Mater. Res.*, 1993, **27**, 183–189.
16 L. D. Harris, B. S. Kim and D. J. Mooney, *J. Biomed. Mater. Res.*, 1998, **42**, 396–402.
17 W. L. Murphy, R. G. Dennis, J. L. Kileny and D. J. Mooney, *Tissue Eng.*, 2002, **8**, 43–52.
18 L. Kang, B. G. Chung, R. Langer and A. Khademhosseini, *Drug Discovery Today*, 2008, **13**, 1–13.
19 Y. Du, E. Lo, M. K. Vidula, M. Khabiry and A. Khademhosseini, *Cell. Mol. Bioeng.*, 2008, **1**, 157–162.
20 J. W. Nichol and A. Khademhosseini, *Soft Matter*, 2009, **5**, 1312–1319.
21 K. M. Ainslie and T. A. Desai, *Lab Chip*, 2008, **8**, 1864–1878.
22 M. Hu, R. Deng, K. M. Schumacher, M. Kurisawa, H. Ye, K. Purnamawati and J. Y. Ying, *Biomaterials*, 2010, **31**, 863–869.
23 T. Takei, N. Kishihara, S. Sakai and K. Kawakami, *Biochem. Eng. J.*, 2010, **49**, 143–147.
24 S. Shin, J. Y. Park, J. Y. Lee, H. Park, Y. D. Park, K. B. Lee, C. M. Whang and S. H. Lee, *Langmuir*, 2007, **23**, 9104–9108.
25 C. M. Hwang, Y. Park, J. Y. Park, K. Lee, K. Sun, A. Khademhosseini and S. H. Lee, *Biomed. Microdevices*, 2009, **11**, 739–746.
26 K. H. Lee, S. J. Shin, C. B. Kim, J. K. Kim, Y. W. Cho, B. G. Chung and S. H. Lee, *Lab Chip*, 2010, **10**, 1328–1334.
27 E. Kang, S. J. Shin, K. H. Lee and S. H. Lee, *Lab Chip*, 2010, **10**, 1856–1861.
28 M. Marimuthu, S. Kim and J. An, *Soft Matter*, 2010, **6**, 2200–2207.
29 W. Jeong, J. Kim, S. Kim, S. Lee, G. Mensing and D. J. Beebe, *Lab Chip*, 2004, **4**, 576–580.
30 J. H. Jung, C. H. Choi, S. Chung, Y. M. Chung and C. S. Lee, *Lab Chip*, 2009, **9**, 2596–2602.
31 E. Tumarkin and E. Kumacheva, *Chem. Soc. Rev.*, 2009, **38**, 2161–2168.
32 W. J. Jeong, J. Y. Kim, J. Choo, E. K. Lee, C. S. Han, D. J. Beebe, G. H. Seong and S. H. Lee, *Langmuir*, 2005, **21**, 3738–3741.
33 H. J. Oh, S. H. Kim, J. Y. Baek, G. H. Seong and S. H. Lee, *J. Micromech. Microeng.*, 2006, **16**, 285–291.
34 W. H. Tan and S. Takeuchi, *Adv. Mater.*, 2007, **19**, 2696–2701.
35 D. Dendukuri, T. A. Hatton and P. S. Doyle, *Langmuir*, 2007, **23**, 4669–4674.
36 S. Seiffert and D. A. Weitz, *Soft Matter*, 2010, **6**, 3184–3190.
37 D. Dendukuri, D. C. Pregibon, J. Collins, T. A. Hatton and P. S. Doyle, *Nat. Mater.*, 2006, **5**, 365–369.
38 P. Panda, S. Ali, E. Lo, B. G. Chung, T. A. Hatton, A. Khademhosseini and P. S. Doyle, *Lab Chip*, 2008, **8**, 1056–1061.
39 D. K. Hwang, D. Dendukuri and P. S. Doyle, *Lab Chip*, 2008, **8**, 1640–1647.
40 S. H. Kim, J. W. Shim, J. M. Lim, S. Y. Lee and S. M. Yang, *New J. Phys.*, 2009, **11**, 075014.
41 S. Q. Xu, Z. H. Nie, M. Seo, P. Lewis, E. Kumacheva, H. A. Stone, P. Garstecki, D. B. Weibel, I. Gitlin and G. M. Whitesides, *Angew. Chem., Int. Ed.*, 2005, **44**, 724–728.
42 A. S. Utada, E. Lorenceau, D. R. Link, P. D. Kaplan, H. A. Stone and D. A. Weitz, *Science*, 2005, **308**, 537–541.
43 S. W. Choi, Y. Zhang and Y. N. Xia, *Adv. Funct. Mater.*, 2009, **19**, 2943–2949.
44 B. Y. Kim, L. Y. Hong, Y. M. Chung, D. P. Kim and C. S. Lee, *Adv. Funct. Mater.*, 2009, **19**, 3796–3803.
45 N. Prasad, J. Perumal, C. H. Choi, C. S. Lee and D. P. Kim, *Adv. Funct. Mater.*, 2009, **19**, 1656–1662.
46 R. F. Shepherd, J. C. Conrad, S. K. Rhodes, D. R. Link, M. Marquez, D. A. Weitz and J. A. Lewis, *Langmuir*, 2006, **22**, 8618–8622.
47 J. Yeh, Y. Ling, J. M. Karp, J. Gantz, A. Chandawarkar, G. Eng, J. Blumling, 3rd, R. Langer and A. Khademhosseini, *Biomaterials*, 2006, **27**, 5391–5398.
48 G. T. Franzesi, B. Ni, Y. B. Ling and A. Khademhosseini, *J. Am. Chem. Soc.*, 2006, **128**, 15064–15065.
49 P. Aymard, D. R. Martin, K. Plucknett, T. J. Foster, A. H. Clark and I. T. Norton, *Biopolymers*, 2001, **59**, 131–144.
50 Y. Ling, J. Rubin, Y. Deng, C. Huang, U. Demirci, J. M. Karp and A. Khademhosseini, *Lab Chip*, 2007, **7**, 756–762.
51 J. H. Park, B. G. Chung, W. G. Lee, J. Kim, M. D. Brigham, J. Shim, S. Lee, C. M. Hwang, N. G. Durmus, U. Demirci and A. Khademhosseini, *Biotechnol. Bioeng.*, 2010, **106**, 138–148.
52 M. P. Linnes, B. D. Ratner and C. M. Giachelli, *Biomaterials*, 2007, **28**, 5298–5306.
53 N. A. Peppas, Y. Huang, M. Torres-Lugo, J. H. Ward and J. Zhang, *Annu. Rev. Biomed. Eng.*, 2000, **2**, 9–29.
54 A. P. Golden and J. Tien, *Lab Chip*, 2007, **7**, 720–725.
55 C. J. Bettinger, B. Orrick, A. Misra, R. Langer and J. T. Borenstein, *Biomaterials*, 2006, **27**, 2558–2565.
56 B. M. Gillette, J. A. Jensen, B. Tang, G. J. Yang, A. Bazargan-Lari, M. Zhong and S. K. Sia, *Nat. Mater.*, 2008, **7**, 636–640.
57 M. D. Brigham, A. Bick, E. Lo, A. Bendali, J. A. Burdick and A. Khademhosseini, *Tissue Eng. A*, 2009, **15**, 1645–1653.
58 M. P. Cuchiara, A. C. Allen, T. M. Chen, J. S. Miller and J. L. West, *Biomaterials*, 2010, **31**, 5491–5497.
59 K. H. Lee, S. J. Shin, Y. Park and S. H. Lee, *Small*, 2009, **5**, 1264–1268.
60 C. H. Yeh, P. W. Lin and Y. C. Lin, *Microfluid. Nanofluid.*, 2010, **8**, 115–121.
61 M. Hu, M. Kurisawa, R. Deng, C. M. Teo, A. Schumacher, Y. X. Thong, L. Wang, K. M. Schumacher and J. Y. Ying, *Biomaterials*, 2009, **30**, 3523–3531.
62 J. T. Borenstein, M. M. Tupper, P. J. Mack, E. J. Weinberg, A. S. Khalil, J. Hsiao and G. Garcia-Cardena, *Biomed. Microdevices*, 2010, **12**, 71–79.
63 C. J. Bettinger, E. J. Weinberg, K. M. Kulig, J. P. Vacanti, Y. D. Wang, J. T. Borenstein and R. Langer, *Adv. Mater.*, 2006, **18**, 165–169.
64 P. He, M. Zeng and F. E. Curry, *Am. J. Physiol. Heart Circ. Physiol.*, 2000, **278**, H1124–H1133.
65 R. H. Adamson, B. Liu, G. N. Fry, L. L. Rubin and F. E. Curry, *Am. J. Physiol.*, 1998, **274**, H1885–H1894.
66 K. H. Wong, J. G. Truslow and J. Tien, *Biomaterials*, 2010, **31**, 4706–4714.

67 G. M. Price, K. H. Wong, J. G. Truslow, A. D. Leung, C. Acharya and J. Tien, *Biomaterials*, 2010, **31**, 6182–6189.
68 C. J. Bettinger, K. M. Cyr, A. Matsumoto, R. Langer, J. T. Borenstein and D. L. Kaplan, *Adv. Mater.*, 2007, **19**, 2847–2850.
69 N. W. Choi, M. Cabodi, B. Held, J. P. Gleghorn, L. J. Bonassar and A. D. Stroock, *Nat. Mater.*, 2007, **6**, 908–915.
70 C. P. Huang, J. Lu, H. Seon, A. P. Lee, L. A. Flanagan, H. Y. Kim, A. J. Putnam and N. L. Jeon, *Lab Chip*, 2009, **9**, 1740–1748.
71 W. J. Polacheck, J. L. Charest and R. D. Kamm, *Proc. Natl. Acad. Sci. U. S. A.*, 2011, **108**, 11115–11120.
72 G. Vozzi, C. Flaim, A. Ahluwalia and S. Bhatia, *Biomaterials*, 2003, **24**, 2533–2540.
73 S. Sarkar, G. Y. Lee, J. Y. Wong and T. A. Desai, *Biomaterials*, 2006, **27**, 4775–4782.
74 J. J. Moon, S. H. Lee and J. L. West, *Biomacromolecules*, 2007, **8**, 42–49.
75 C. M. Nelson, M. M. VanDuijn, J. L. Inman, D. A. Fletcher and M. J. Bissell, *Science*, 2006, **314**, 298–300.
76 D. A. Bruzewicz, A. P. McGuigan and G. M. Whitesides, *Lab Chip*, 2008, **8**, 663–671.
77 S. E. Chung, W. Park, S. Shin, S. A. Lee and S. Kwon, *Nat. Mater.*, 2008, **7**, 581–587.
78 Y. Du, E. Lo, S. Ali and A. Khademhosseini, *Proc. Natl. Acad. Sci. U. S. A.*, 2008, **105**, 9522–9527.
79 B. Zamanian, M. Masaeli, J. W. Nichol, M. Khabiry, M. J. Hancock, H. Bae and A. Khademhosseini, *Small*, 2010, **6**, 937–944.
80 J. G. Fernandez and A. Khademhosseini, *Adv. Mater.*, 2010, **22**, 2538–2541.